

1 **The residual mean circulation in the tropical tropopause layer driven by**
2 **tropical waves**

3

4 **David A. Ortland**

5 *NorthWest Research Associates*

6 *4118 148th Ave NE*

7 *Redmond, WA 98052*

8 ortland@nwra.com

9

10 **M. Joan Alexander**

11 *NWRA, CoRA Office*

12

Abstract. We use latent heating estimates derived from rainfall observations to construct model experiments that isolate equatorial waves forced by tropical convection from mid-latitude synoptic-scale waves. These experiments are used to demonstrate that quasi-stationary equatorial Rossby waves forced by latent heating drive most of the observed residual mean upwelling across the tropopause transition layer within 15° of the equator. The seasonal variation of the equatorial waves and the mean meridional upwelling they cause is examined for two full years from 2006 to 2007. We find that changes in equatorial Rossby wave propagation through seasonally varying mean winds is the primary mechanism for producing an annual variation in the residual mean upwelling. In the tropical tropopause layer, averaged within 15° of the equator and between 90-190 hPa, the annual cycle varies between a maximum upwelling of $.4 \text{ mm s}^{-1}$ during Boreal winter and Spring and a minimum of $.2 \text{ mm s}^{-1}$ during Boreal summer. This variability seems to be due to small changes in the mean wind speed in the tropics. Seasonal variations in latent heating have only a relatively minor effect on seasonal variations in tropical tropopause upwelling. We also find that Kelvin waves drive a small downward component of the total circulation over the equator that may be modulated by the quasi-biennial oscillation.

1. Introduction

Recent variations in stratospheric water vapor with unknown causes have been implicated in global decadal-scale surface temperature variations (Solomon et al., 2010). Most notably, a sudden decrease in stratospheric water vapor in 2001 coincided with a cooling in tropical tropopause temperatures observed in radiosondes (Randel and Wu, 2006), and the change persisted and only slowly recovered through the first decade of the 21st century. These decadal-scale changes to both temperature and water vapor suggest that there was an increase in tropical upwelling across the tropical tropopause layer (TTL). In

this paper we define the TTL to be the layer between 90-190 hPa (13-17 km). The tropical upwelling circulation is driven by waves and deep convection and stratospheric water is further controlled by tropopause temperatures. Hence it is natural to suspect that there is an increase in wave driving, either through enhanced wave forcing or through changes in the pattern of wave propagation that would lead to enhanced wave-flux divergence. Although extratropical wave pumping clearly influences the zonal mean tropical upwelling in the lower stratosphere (Holton et al., 1995), several recent studies have found that global-scale equatorial waves, forced by convection, play an important role in modulating tropical tropopause temperatures and upwelling in the tropopause layer that control stratospheric water vapor (Boehm and Lee, 2003; Kerr-Munslow and Norton, 2006; Norton, 2006; Ryu and Lee, 2010; Grise and Thompson, 2013).

Tropical upwelling across the TTL is part of a wave driven (Brewer-Dobson) circulation, and is the region where dehydration of air entering the stratosphere occurs. In this paper we shall quantify mean upwelling in terms of the residual mean vertical velocity. Plumb and Eluszkiewicz (1999) showed that the steady component of the residual mean vertical velocity at the equatorial TTL can only be driven by EP-flux convergence within 20° of the equator in the lower stratosphere. However, Randel et al. (2002) found that transient mid-latitude EP-flux divergence from extra-tropical waves can drive transient upwelling at the equator. The waves that contribute to the TTL upwelling may include synoptic scale transient eddies, extratropical stationary planetary waves (Scott, 2002), gravity waves (Garcia and Randel, 2008; Li et al., 2008; McLandress and Shepherd, 2009; Calvo et al., 2010; Sigmond and Scinocca, 2010) and tropical waves forced by convective heating. It is important to determine the role each of these waves may play in the tropical upwelling so that the causes of variability and long-term trends may be more easily identified. It is also important to distinguish variability in forcing from variability that arises from changes in wave propagation due to the mean state variability (Garcia and Randel, 2008; Calvo et al., 2009). Tropical upwelling rates

have been obtained from several studies. Schoeberl et al. (2008) used MLS and HALOE water vapor measurements to determine upwelling rates of .4-.5 mm/s at 17 km (~100 hPa). Dima and Wallace (2007) used ERA-40 reanalysis to determine an annual mean vertical velocity of .55 mm/s. Abalos et al. (2012) derive upwelling rates by several methods using ERA-interim data, which show an annual cycle with amplitude of approximately a factor of two with a minimum in July of ~.25 mm/s and maximum in January of ~.5mm/s

It is uncertain which wave type is primarily responsible for driving tropical upwelling. Boehm and Lee (2003) proposed that tropical waves may be important. Kerr-Munslow and Norton (2006) used ECMWF reanalysis (ERA-15) at 90hPa and deduced that tropical waves made a significant contribution to tropical upwelling. Randel et al. (2008) found that there is an equal contribution to upwelling from both tropical and extratropical waves in ERA-40, and that both tropical and extratropical waves can contribute to the seasonal cycle. They speculate that in the case of tropical waves, this is due to changes in the seasonal pattern of stationary heating. The recent review by Randel and Jensen (2013) mentions that the mechanisms driving the annual cycle in TTL temperatures and upwelling remain to be clarified. Grise and Thompson (2013) found evidence for tropical wave driving of week-to-week variability in TTL upwelling, but results for longer timescales were inconclusive. Deckert and Dameris (2008) found that higher SSTs in the CCM E39/C amplify deep convection, which is correlated in the model with anomalous production of quasi-stationary equatorial waves. (We define quasi-stationary waves here as stationary waves plus waves with low frequency that travel westward relative to the mean flow.) Anomalous EP-flux divergence associated with the quasi-stationary wave anomaly was shown to drive an anomalous low-latitude Brewer-Dobson cell that was responsible for an increase in ozone-poor air of the model lower stratosphere.

We attempt to quantify the upwelling driven by equatorial waves, particularly equatorial Rossby waves. Our model simulations are forced using latent heating estimates derived from TRMM rainfall data. Our experiments are designed to remove as much as possible the effects that extra-tropical synoptic-scale waves have on tropical upwelling so that the effects of tropical waves forced by latent heating can be quantified separately. These experiments show that the observed annual mean velocity and temperature field pattern can be reproduced using wave forcing from latent heating alone. The tropical upwelling driven by the quasi-stationary waves in our experiments closely match the upwelling derived from observations. Our experiments further show that the annual cycle in upwelling is not caused by seasonal changes in equatorial wave sources. Instead, the annual cycle in upwelling results primarily from seasonal changes in wave propagation caused by the annual cycle in tropical zonal-mean winds. We shall also examine the separate contributions to upwelling from synoptic, stationary, eastward, and westward waves, and examine mechanisms, such as the quasi-biennial oscillation (QBO), that may give rise to interannual variability in upwelling.

2. Model description

a) Transformed Eulerian-Mean equations

The focus of this paper is on the wave-driven vertical transport velocity across the TTL. This velocity is estimated using the residual mean meridional circulation (RMMC), which is part of the Transformed Eulerian-Mean (TEM) formalism. The RMMC velocities are good approximations to Lagrangian-Mean transport velocities when the waves have small amplitude, are steady, and adiabatic. These conditions are reasonable to assume, but it is beyond the scope of this paper to check their validity. A good reference for the TEM formalism and its use for estimating transport is provided by Andrews et al. (1987), Chapters 3 and 9.

The TEM equations have the same form as the Eulerian-Mean equations except that eddy fluxes have been combined into mean meridional circulation components and forcing terms. In addition to thermal wind balance (not displayed), the zonal momentum, thermal energy, and continuity equations express the balance between the RMMC (\bar{v}^* , \bar{w}^*), the time tendency of the zonal mean zonal wind and temperature, and various forcing mechanisms due to eddies, dissipation, and heating:

$$\begin{aligned} \bar{u}_t + \bar{v}^* \left[(a \cos \phi)^{-1} (\bar{u} \cos \phi)_\phi - f \right] + \bar{w}^* \bar{u}_z &= (\rho_0 a \cos \phi)^{-1} \nabla \cdot \mathbf{F} + X; \\ \bar{T}_t + a^{-1} \bar{v}^* \bar{T}_\phi + \bar{w}^* R^{-1} H N^2 &= Q; \\ (a \cos \phi)^{-1} (\bar{v}^* \cos \phi)_\phi + \rho_0^{-1} (\rho_0 \bar{w}^*)_z &= 0. \end{aligned} \quad (1)$$

The RMMC may be expressed in terms of the Eulerian mean and wave fields, but we will not need the formulae here. The RMMC is calculated instead as a part of the solution to (1). The terms in the equations are zonal wind u , temperature T , Coriolis parameter f , scale height H (7 km), gas constant R , density ρ , earth radius a , and buoyancy frequency N . Zonal mean is denoted with an over-bar. Derivatives with respect to time t , latitude ϕ , and log-pressure altitude z are denoted with a subscript. These equations are forced by the divergence of the Eliassen-Palm (EP) flux vector:

$$\begin{aligned} F^{(\phi)} &= \rho_0 a \cos \phi \left(\bar{u}_z \left(\overline{v' T'} \right) R (H N^2)^{-1} - \left(\overline{v' u'} \right) \right), \\ F^{(z)} &= \rho_0 a \cos \phi \left\{ \left[f - (a \cos \phi)^{-1} (\bar{u} \cos \phi)_\phi \right] \left(\overline{v' T'} \right) R (H N^2)^{-1} - \left(\overline{w' u'} \right) \right\} \end{aligned} \quad (2)$$

Contributions to the heating term Q include radiative and wave heating/cooling. Parameterized dissipative mechanical forcing is denoted by X .

The TEM equations describe how upwelling in the TTL is produced by EP-flux divergence. We will show that the typical wave forcing pattern consists of two subtropical regions where $\nabla \cdot \mathbf{F} < 0$. This is mainly balanced by the Coriolis term on the left side of the zonal momentum equation. In a nearly steady state solution, the time-tendency of zonal wind is essentially zero except very close to the equator. Since the

Coriolis parameter changes sign across the equator, the TEM meridional wind must also change sign across the equator. By the continuity equation, the resulting meridional gradient in the meridional wind is balanced by a negative vertical gradient in upwelling, hence the peak upwelling lies below the centers of maximum EP-flux convergence. The thermal energy equation says that in a nearly steady state this upwelling must be balanced by radiative heating.

b) Primitive Equation Model

All calculations are performed with a time dependent primitive equation model. The model fields are represented by a spherical harmonic expansion with triangular truncation T40. A higher horizontal resolution has no effect on the wave spectrum due to limits on the frequencies resolved in the forcing (Ortland et al. 2011). The vertical log-pressure altitude grid extends from the surface to 60 km with 750 m spacing. Rayleigh friction above 40 km acts on the wave components to prevent wave reflection from the upper boundary. Newtonian cooling with a rate of $.05 \text{ d}^{-1}$ above the tropopause damps the waves and relaxes the zonal mean temperatures of the model to climatological values described below. Waves in the model are forced by heating derived from gridded global TRMM rainfall rate data sampled every three hours (Huffman et al. 2007). The heating is also computed at 3-hourly intervals and interpolated to intermediate model time steps. The heating is tapered to zero poleward of 30° , so the wave response can be interpreted to consist primarily of tropical waves. The vertical heating profiles include both convective and stratiform rain contributions. The zonal mean heating is removed from the forcing introduced into the model since we are not interested in examining the Hadley circulation and the influence it has on zonal mean winds and temperatures. A full description of how the latent heating is derived from TRMM is given in Ryu et al (2011). The Ryu et al. (2011) study examines transient tropical waves in the stratosphere forced by latent

heating derived from TRMM in this way, and provides further details on the model and wave spectra. The primary focus of the present paper is on the seasonally-varying model response in the upper troposphere and lower stratosphere to the waves forced by this 3-hourly varying heating, but the waves of primary interest for this study are the quasi-stationary waves.

Monthly and zonally averaged zonal winds and temperatures derived from observations are used to define the zonal mean background for the model. The observed values (OBS) were obtained from NCEP reanalysis (Kalnay et al., 1996). The NCEP monthly zonal mean zonal wind values in the troposphere and lower stratosphere were compared to values obtained from Modern-Era Retrospective Analysis (MERRA) and differences were found to be less than 1 ms^{-1} in the upper troposphere and lower stratosphere. These monthly averages were further modified (MOD) as described below. The MOD values are assigned to the midpoint of each model month, and the value used in the model is obtained by linear interpolation to the current model time step. The model zonal mean winds are relaxed to these interpolated values at a rate of $.1 \text{ d}^{-1}$ throughout the domain outside the tropics and at a rate of $.5 \text{ d}^{-1}$ within 30° of the equator. This relaxation rate was required to keep the model zonal mean within 1 ms^{-1} of observations in the tropics. Since the zonal and monthly mean subtropical tropospheric jets are baroclinically unstable, synoptic scale Rossby waves are spontaneously generated in the model when the observed winds and temperatures are used. In order to examine only the waves generated by tropical heating, the MOD values were designed to suppress the spontaneous generation of synoptic waves. The MOD background and TRMM heating from January 2005 through December 2007 is used to produce a multi-year control run (CTRL). The first year is not examined here, and is used for a ramp-up.

To construct the MOD background that suppresses synoptic waves, the model is initialized with the OBS values of wind and temperatures for each month plus a random wave disturbance. It is then allowed to run freely for 90 days with no TRMM heating

and with no relaxation to the zonal mean, while synoptic scale waves develop and modify the mean flow into a stable configuration. This duration is long enough for the transient synoptic waves to complete their modification, die off due to the Newtonian cooling and the sponge, and produce a steady zonal mean ‘relaxed’ state (RLX) plus weak quasi-stationary waves. The MOD background is then obtained by merging the RLX and OBS zonal mean fields. The merge retains OBS within 20 degrees of the equator, with a smooth transition to RLX poleward of 35 degrees. Since most of the baroclinic instability arises at mid-latitudes, this modification retains a state that is nearly stable to baroclinic waves, and also retains the tropical zonal mean background state, which is important for producing realistic propagation of the tropical waves forced in the model. The MOD and OBS backgrounds are identical to each other out to 20° and within a few m/s of each other out to about 50° from the equator. The main differences are poleward of 50°. The jet core of MOD is poleward of OBS and has a larger magnitude. We do not expect the equatorially confined tropical waves to be sensitive to the winds poleward of 50°.

Two experiments were run to test that the MOD state suppresses the baroclinic waves. In both, the model was initialized with a random disturbance and no tropical waves are forced. However, unlike the simulation that produced the RLX state, the model was constrained to the zonal mean zonal wind with relaxation rates used in CTRL. In the first ‘synoptic run’, the zonal mean background is relaxed to OBS, while in the second ‘modified synoptic run’ the mean background is relaxed to the MOD state. Both simulations generate synoptic scale waves that persist for a 3-year duration. However, in the modified case the synoptic waves are smaller by a factor of 5. The amplitude of synoptic waves in this second run is also negligible compared to the tropical waves generated in CTRL, which is the result we are trying to achieve.

We will also look at simulations where the background zonal mean zonal wind is relaxed to zero (UBR0) using the same relaxation rates as in CTRL. The zonal mean

temperatures in UBR0 are set equal to a climatological vertical profile obtained from observations by averaging between 20°N to 20°S. Using zero background winds rather than climatological zonal mean zonal winds also insures that synoptic scale waves do not form on the subtropical jets. Comparing UBR0 and CTRL simulations will enable us to determine the effect that the zonal mean winds have on the wave propagation.

c) TEM model

Our goal is to calculate the component of the RMMC that is forced by the tropical waves. The zonal mean meridional circulation of the CTRL simulation cannot be used for this purpose because the relaxation of the model zonal mean in the CTRL and UBR0 simulations severely suppresses that circulation. What we do instead is to compute the EP flux and divergence from the CTRL and UBR0 simulations, then force a zonal mean version of the primitive equation model with this EP-flux divergence. Forced in this way, but without the same relaxation to the zonal mean as in the wave model, the zonally symmetric version of the primitive equation model solves the TEM equations (1) and the meridional and vertical wind fields can be interpreted as the RMMC. The TEM model is run separately for each month. The RMMC becomes steady in about 30 days. This results in an estimate of the RMMC for each month of the 2-year simulation. Averages of three consecutive months give the seasonal estimates shown below.

The zonal momentum forcing in the TEM model is determined by first calculating the zonal wavenumber-frequency spectra of all fields in the control run by using monthly stretches of the model output. The spectral components of each field are then used to calculate the EP-flux divergence spectrum. Following sections describe results when the model is forced with the total spectrum, or the sum of eastward, westward, or stationary parts of this spectrum. The TEM model also retains the Newtonian cooling used in the full wave model simulations. This is represented by the heating term Q in equations (1).

It was found that wave heating has negligible effect on the upwelling in the TTL and hence is not included as a forcing term of the TEM model.

The TEM model is initialized with the monthly and zonal mean zonal winds from the 3D simulations, however we found that the RMMC calculated in the model did not depend on these background winds. Although the RMMC becomes steady in about 30 days, the zonal wind in the TEM model is not steady, because important tropospheric forcing mechanisms are absent in the simplified model. To help control these tendencies in a way that does not affect the RMMC upwelling in the TTL, the zonal wind is relaxed to the initial state only below 10 km, at a rate of $.1 \text{ d}^{-1}$. This relaxation forcing is represented by the X term in equations (1). However, the fact that the zonal wind in the TEM model slowly evolves does not affect the RMMC results. Despite continuous evolving zonal winds, the RMMC remains steady for as long as 90 days or more.

To determine that the TEM model produces a reasonable estimate of residual mean upwelling, the balance of terms in the TEM equations was examined. It was found that the primary balance in the TEM zonal momentum equation is between the EP-flux divergence and the Coriolis term. The advection terms are negligible within 30° of the equator. Hence the structure of the zonal mean winds in the TEM model has no effect on the RMMC in the tropics. The relaxation forcing X had only a small contribution below 10 km. The zonal wind tendency is also a negligible part of the balance in most cases except in those months where there is some non-zero EP-flux divergence on the equator. However, this tendency also does not affect the residual mean upwelling – it balances a component of the residual mean meridional wind that is symmetric about the equator. This symmetric component of the meridional wind has very small horizontal gradient, hence does not contribute to upwelling through the continuity equation. This was verified by running the TEM model forced by EP-flux divergence that was modified to be zero within 5° of the equator. These test simulations had the same residual mean upwelling as produced by unmodified EP-flux divergence, and also had negligible zonal

wind tendency in the tropics. The balance in the TEM thermal energy equation for all months is between the adiabatic term and Newtonian relaxation and the temperature tendency in the tropics is negligible. Hence the TTL upwelling that we derive is an accurate estimate of the TEM response to tropical wave EP-flux convergence isolated from extratropical wave influences.

3. Residual mean circulation

a) Heating and mean response

Since we will be looking at seasonal variations in the RMMC, it is worth looking first at the seasonal variations in the heating pattern. The latent heating derived from TRMM is averaged over the 2007 seasons and shown in Figure 1. Large regions of heating occur over Africa, Southeast Asia, and South America. Heating amplifies in the summer hemisphere, with the largest magnitude occurring in the DJF season. A band of heating north of the equator is associated with the intertropical convergence zone. This band migrates in latitude with season. The variation in the heating configuration will be seen to produce a seasonal variation in the wave fluxes that is not readily apparent in the EP-flux divergences or the RMMC response.

We first demonstrate that our simulation produces a realistic stationary wave structure in the tropics in response to the TRMM heating by comparing our simulation to observations presented by Dima and Wallace (2007). Figure 2 shows the results from the control run averaged over the year 2007. The top two panels show the perturbation temperature field with color-shaded contours and the wind field in the plane of the figure with vectors, while the bottom panel shows actual temperatures. The vertical wind components have been scaled by a factor of 1000 so that they are visible. The TTL in this and other figures is marked with red boundary lines. The top panel of Fig. 2 is obtained by averaging over all latitudes within 10° of the equator. Positive vertical

298 velocities mainly occur over deep convective cloudy regions in the western Pacific, while
299 down-welling occurs over clear sky regions. The coldest temperatures occur within the
300 TTL over the upwelling. Our simple model produces a pattern of wind velocities and
301 temperature anomalies above 450 hPa that is very similar in structure and magnitude to
302 that found by Dima and Wallace (2007) in ERA-40 data (their Fig. 5). The bottom panel
303 of Fig. 2 shows temperatures at 100 hPa averaged over 2007 as function of longitude and
304 latitude. It illustrates the western Pacific cold pool, centered between 130°-190°
305 longitude over the equator, with lobes extending westward in the subtropics. In our
306 model this is produced exclusively as part of the stationary Rossby wave pattern. It
307 agrees very well with the ERA-40 data for roughly the same period shown by Virts et al.
308 (2010) (their Fig. 3). We may conclude that tropical waves driven by the spatial
309 variability in the latent heating are primarily responsible for driving observed
310 longitudinal variations in the circulation in the TTL. The structure of the temperatures is
311 also similar in other years of our run.

312 The middle panel of Fig. 2 shows the wave structure in the longitude-latitude
313 plane at 260 hPa (10.5 km) averaged over 2007. The temperature anomalies display the
314 structure of a superposition of several Rossby waves (e.g. Gill, 1980). The Rossby wave
315 symmetric modes represent the response to the component of the heating symmetric
316 about the equator. They have a primary peak away from the equator and a local
317 minimum at the equator, even if the peak heating occurs on the equator. Note that the
318 temperature anomaly is primarily asymmetric about the equator just west of the
319 Greenwich meridian, while it is symmetric elsewhere. This annual mean pattern is also
320 persistent from year to year in the model simulation. These patterns are very similar to
321 the streamfunction response to annually averaged latent heating shown in Schumacher et
322 al. (2004) (their Fig. 5).

323

b) Seasonal structure

We next examine the EP-flux from the full tropical wave spectrum and its divergence, averaged over the four seasons of 2007. Figure 3 shows the result for the UBR0 simulation in the panels on the left and the results for CTRL simulation on the right. The EP-flux is shown by scaled vectors and the flux divergence is shown with colored contours. In all panels of Fig. 3 we see two regions of EP-flux convergence on either side of the equator centered close to 100 hPa. It is this convergence that drives the RMMC upwelling through the TTL over the equator, as explained in Section 2a. The EP-flux convergence is more asymmetric about the equator during solstice, with larger magnitude in the summer hemisphere in which the peak heating occurs, as shown in Figure 1.

One can see several differences in EP-flux convergence near the tropopause in the two simulations that is caused by the mean zonal winds. First, in the CTRL simulation the convergence is more confined equatorward of 30° than in the UBR0 simulation. This is probably due to the tropical confinement of the stationary Rossby waves by the strong westerlies in the subtropical jets. Second, the CTRL convergence is stronger in general, but particularly so in DJF. As we shall see below, this is the cause of the seasonal variability of the RMMC. Third, for the JJA and SON seasons, the convergence pattern is lower in CTRL than in UBR0, and there are strong regions of EP-flux divergence over the equator. This is possibly related to the arrival of the westward phase of the quasi-biennial oscillation (QBO) in the lower stratosphere at this time. For the DJA and MAM seasons there is a weak remnant of the eastward phase of the QBO just above the tropopause. The westward QBO winds confine the Rossby waves slightly lower in the TTL and allow the propagation of Kelvin waves into the stratosphere. The dissipation of Kelvin waves produces the weak positive EP-flux divergence seen directly over the equator in the TTL in the last two seasons of 2007. These features will be further discussed in the following subsections.

The EP-flux divergences shown in Fig. 3 are used to force the zonally symmetric TEM model as described in Section 2c. The mean meridional and vertical winds calculated in this way give the RMMC, which provide an estimate for the zonal mean transport velocity. The RMMC's that result from the EP-flux divergences calculated from the UBR0 and CTRL simulations are shown in the left and right columns, respectively, of Figure 4. These Figures use scaled vectors for the RMMC and color contours showing the residual mean vertical velocity. The EP-flux convergence on either side of the equator in the TTL gives rise to two circulation cells with rising motion over the equator and sinking motion in the subtropics.

The circulation pattern for each season shown for the UBR0 simulation in Fig. 4 is nearly symmetric about the equator, and except for DJF07, the vertical velocity is maximum over the equator. The deviation from symmetry about the equator in the circulation results from the asymmetry of the heating about the equator. The local minimum in the vertical velocity over the equator for DJF07 will be discussed below. Comparing the left and right columns, we note that the inclusion of background winds produces considerable asymmetry in the circulation, and both weakens the circulation pattern somewhat and lowers that altitude of maximum vertical velocity by about 1 km. The sensitivity of the RMMC to the structure of the mean winds suggests a mechanism for controlling the seasonal and interannual variation in the RMMC that will be examined further below. In our model the seasonally averaged value of the residual mean vertical velocity at 111 hPa over the equator is between .3 and .6 mm s⁻¹. This is roughly consistent with observational estimates (Schoeberl et al. 2008; Dima and Wallace 2007; Randel et al., 2008; Abalos et al., 2012). The strength of the circulation varies throughout the year.

c) Variability

The seasonal variation in the upwelling through the TTL will depend on the variability of the heating, as shown in Fig. 1, and on the variability of the zonal mean basic state through which the tropical waves propagate. We shall explore which mechanisms are responsible for producing variability in the upwelling by making a comparison between the CTRL and UBR0.

The observed tropical zonal mean winds for 2006-2007 are shown in Figure 5. The top panel shows monthly and latitudinally averaged zonal mean zonal wind up to 30 km. The bottom panel shows the zonal mean zonal winds averaged over the TTL. Both panels show weak, but significant, variability in the upper troposphere. Weak easterly wind speeds on the order of $5\text{-}10\text{ ms}^{-1}$ develop from June through November, while weak westerly wind speeds less than 5 ms^{-1} prevail at other times. Manabe et al. (1974) first described this variability with a general circulation model. The tropospheric jets strengthen and extend into the subtropics of the winter hemisphere, and weaken and retreat into the summer hemisphere. In the stratosphere, the westerly phase of the quasi-biennial oscillation (QBO) descends to the top of the TTL between October 2006 and July 2007. Easterly winds lie above the TTL at all other times.

The variation of the vertical component of EP-flux, shown in Figure 6, indicates how the background winds affect wave propagation. The left panels of the figure show results of the CTRL simulation and the right panels show results from the UBR0 simulations. The top panels show the time evolution of the vertical profiles of vertical EP-flux at the equator and the bottom panels show latitudinal cross sections in the TTL. In the CTRL simulation we see that the upward flux is essentially zero in the tropics during northern summer. When the background winds are set to zero there is still significant wave propagation in the tropics during this period, so we can conclude that the modulation of wave flux is due to background winds and not due to variability in the latent heating wave source. Notice that the reduced vertical wave flux occurs at the time

when weak zonal mean easterly winds prevail in the tropical troposphere. These tropical easterlies inhibit the propagation of Rossby waves, as we might expect. The seasonal variation of the latent heating does produce modulation of wave flux in the subtropics, with maximum flux in the summer hemisphere, as seen by comparing the bottom panels of Fig. 6. Apparently the extension of tropical easterlies into the northern summer subtropics also acts to reduce the subtropical wave flux.

The modulation of wave flux due to variations in heating and wave propagation leads to a modulation of the EP-flux divergence, and hence a modulation of the RMMC. The variability of the EP-flux divergence in our model simulations is shown in Figure 7. The pattern of variability in the vertical profiles of the divergence in the tropics (top panels) closely resembles the variability in the flux profiles. Once again, the mean winds produce a regular seasonal variability in the EP-flux divergence which minimizes between June and October. The latitude structure of the divergence (bottom panels) also has a strong seasonal variation when observed background winds are used in the model, but the variability is much weaker when the background winds are zero.

The modulation of EP flux divergence leads to the modulation of the RMMC shown in Figure 8. There is considerable variability in the upwelling that can be attributed to heating alone (right panels for the UBR0 simulation). Although there is a seasonal pattern evident in the vertical component of EP flux in the UBR0 simulation (Fig. 6, right panels), that pattern is not evident in the upwelling. There is considerable variability in the vertical velocity in this two year simulation, but it is not clear whether this variability is part of a regular seasonal pattern. However, there is a clear seasonal variation in the upwelling for the CTRL simulation that use observed mean winds (left panel). The weak tropical easterlies, as pointed out above, suppress Rossby wave propagation (and enhance Kelvin wave propagation) from June to October and hence this is also the period when the upwelling is weakest. The maximum upwelling during Boreal winter and Spring, averaging around $.8 \text{ mm s}^{-1}$ is a factor of two larger than the minimum

of around $.4 \text{ mm s}^{-1}$ from June to October. The mean winds also significantly alter the latitude structure of the upwelling. The peak upwelling through the TTL occurs in the subtropics of the summer hemisphere. There also appear to be enhancements of the upwelling due to anomalies in the heating structure. For example, upwelling in both simulations is strongest during January 2007.

d) Spectral decomposition

As described in Section 2, the wave fields over each of the seasonal 3-month intervals in the CTRL and UBR0 multi-year model simulations were decomposed into frequency components using the fast Fourier transform, from which the EP-flux divergence for each separate frequency was calculated. In the previous subsection the response to the sum of all frequencies was examined. In this subsection we examine the response to forcing the TEM model with the separate contributions from stationary, eastward, or westward traveling waves. In this spectral decomposition over the 3-month interval, ‘stationary’ waves have periods greater than 90 days. This decomposition turns out to be considerably different for the CTRL and UBR0 simulations. The differences illustrate the effect that the mean winds have on wave propagation. Since the tropical waves responsible for driving the RMMC have phase speeds that are comparable to the wind speeds in the tropics and subtropics, it is not surprising that the EP-flux divergence pattern is sensitive to the mean winds.

The EP-flux and divergence for the DJF07 season, decomposed into stationary, westward, and eastward propagating waves are shown in Figure 9. The CTRL simulation is on the left and the UBR0 simulation is on the right. As we have seen, the wave heating source was confined primarily in the southern hemisphere (Fig. 1), the mean winds (Fig. 5) have magnitude $\sim 5 \text{ ms}^{-1}$ or less in the tropics, (westward in the lower troposphere, eastward in the upper troposphere), and the subtropical jet is much stronger in the

northern hemisphere (30 ms^{-1}) than the southern hemisphere (15 ms^{-1}). Thus we see, for stationary and westward waves in both simulations, the EP flux emanating upward from the southern tropics and subtropics, with some propagation toward and across the equator. For the CTRL simulation the strong northern subtropical jet appears to allow eastward wave propagation out of the northern hemisphere as well. Relative to the UBR0 simulation, the CTRL simulation has increased the EP flux divergence for stationary and eastward waves and decreased the divergence for westward waves. The decrease in westward wave flux is likely a manifestation of the Charney-Drazin criterion (Charney and Drazin, 1961) – the subtropical jets have mean wind speed that is too large for propagation of the Rossby waves that are excited. The nonzero mean winds also allow for Rossby waves that propagate eastward relative to the ground but westward relative to the mean flow.

The eastward wave spectrum also contains Kelvin waves. The EP-flux of Kelvin waves point downward over the equator (since by (2) F_z is upward flux of westward momentum) and, when dissipating, will produce a positive EP-flux divergence. There is a similar region of positive EP-flux divergence and downward flux for eastward waves in both simulations. The Kelvin waves present in these simulations have larger phase speeds than the Rossby waves, and are less affected by the relatively small mean wind speeds in the tropical troposphere.

The RMMC that is driven by the EP-flux divergences for the various wave components from the CTRL and UBR0 simulations are shown in Figure 10. The relative strengths of the residual mean vertical velocity are essentially the same as the relative strengths of the EP-flux divergences shown in Fig. 9. The upwelling driven by stationary waves (Fig 10, top) is stronger in the CTRL than in the UBR0 simulation. The EP-flux divergence pattern for CTRL is shifted poleward from the divergence pattern for UBR0. Thus, the upward residual mean velocity is shifted with a maximum that lies south of the equator. Conversely, the upwelling driven by westward waves (Fig 10, middle) is weaker

in CTRL than in UBR0 due to the suppression of westward Rossby wave propagation. The Kelvin waves (Fig. 10, bottom) force downward residual mean velocity over the equator. This is most evident in UBR0, whereas eastward Rossby waves are also present in CTRL. The upwelling driven by the eastward Rossby waves largely cancels the downwelling driven by the Kelvin waves in this case. Since the downward residual mean velocity driven by the Kelvin waves is more narrowly confined to the equator than the upward velocity driven by the Rossby waves, the total RMMC obtained from the superposition of wave components may actually show a local minimum over the equator. Such a local minimum is evident in the residual mean vertical velocities shown for DJF07 in Fig. 4.

e) Interannual variability

The QBO may influence the RMMC by affecting the waveguide for the tropical waves. The CTRL simulation includes both phases of the QBO. The mean winds shown in Fig. 5 have a QBO westerly phase overlying the TTL from August 2006 through June 2007. The question is whether the QBO signal penetrates deep enough to influence the TTL wave propagation in a significant manner.

There may be interannual variability in the TRMM heating that is used to force waves in our model. To determine if the interannual variability in the RMMC of the CTRL simulation is directly related to wave propagation through the QBO winds, we performed an additional experiment. The model was run using winds from 2006 and TRMM heating from 2007, and conversely, using winds from 2007 and TRMM heating from 2006. Any difference between these runs and the CTRL simulation can only be attributed to a change in the background winds and temperatures.

Examination of the four cross sections of EP-flux and RMMC in each season for each of the cases of 2006/2007 TRMM heating paired with 2006/2007 winds (not shown

here) did not demonstrate convincing differences amongst them that can definitely be attributed to differences in QBO tropical winds. This is not surprising – if one covers the top panel of Fig. 5 with their hand to block out winds above the TTL, it is difficult to discern a QBO pattern in the winds below. Based on the EP-fluxes and divergences shown in previous figures, we note that Rossby waves do not propagate much higher than the TTL.

However, Kelvin waves can readily propagate into the QBO easterly phase, so it is possible that there is a difference in the Kelvin wave signature in the RMMC. From what was discussed above, the Kelvin waves drive a downward circulation over the tropics, potentially forming a local minimum in the RMMC over the equator. There does seem to be a QBO signal in such a Kelvin wave contribution to the RMMC pattern. Figure 11 shows the vertical residual mean velocity averaged over the TTL for the four separate pairings of mean winds and heating in our model runs. The two solid curves in the figure are obtained using observed winds from SON 2006 when QBO westerly winds are in the lower stratosphere. These two curves, produced using TRMM heating from different years, have a noticeable local minimum over the equator, indicating that a circulation driven by dissipating Kelvin waves is present. The dashed curves, obtained using observed winds from 2007 show a depression over the tropics of much smaller magnitude. A plausible explanation for this is that the westerlies present in 2006 inhibit some Kelvin waves from propagating higher into the stratosphere, causing them to dissipate just above the TTL and producing a significant contribution to positive EP-flux divergence.

f) Contributions to upwelling from synoptic waves

Finally, we compare the magnitude of the upwelling in the TTL driven by tropical waves to the upwelling driven by synoptic waves. Synoptic waves in our model grow off

an unstable configuration of the zonal mean subtropical jet, but the strength of these waves depend on how strongly we clamp the model background winds to the observed zonal means. All studies using our model showed that synoptic waves make a small contribution to upwelling through the TTL. However, our model does not incorporate most of the physical processes in the troposphere, so it is difficult to verify the validity of our simulations of synoptic wave dynamics. Here instead the MERRA 3-hourly assimilated product for 2006-2007 is analyzed following the approach already described. Namely, we calculated the EP-flux divergence spectrum for each month, which was then used to force the TEM model to calculate the RMMC response. To isolate the synoptic waves as much as possible, we used only the transient portion of the spectrum – all waves with period less than 30 days. We assume that most of these waves are synoptic, although the results of Section 3d above show that a portion of the transient wave spectrum arises from tropical waves forced by latent heating. Even without being able to make a clean separation between synoptic and tropical waves using MERRA analysis, we obtain the same conclusion as with our own model simulations, that synoptic waves make a negligible contribution to TTL upwelling.

The monthly average of the upwelling calculated using the TEM model forced with the EP-flux divergence from MERRA transient waves is shown in the top panel of Figure 12. Compared to the residual vertical mean velocities shown in the upper left panel of Fig. 8, the upwelling forced by MERRA transient waves is weaker than what is forced by tropical waves by a factor of two or more. Also, the altitude where the peak magnitude occurs is shifted lower into the troposphere. Upwelling in the TTL forced by synoptic waves is estimated to be less than .2 mm/s. We see that synoptic waves primarily contribute to upwelling into the lower part of the TTL whereas tropical waves are far more effective at producing upwelling all the way through the TTL. It is also interesting to note that the upwelling forced by the MERRA transient waves has a semi-annual variation that peaks near equinox and has a minimum during solstice.

The EP-flux divergence for MERRA transient waves and the RMMC obtained from the TEM model for SON 2007 are shown in the middle and bottom panels of Fig. 12, respectively. Compared to Figs. 3 and 4, the peak in the transient wave EP-flux convergence has similar magnitude, but occurs 5 km lower than and around 5° poleward of the tropical wave EP-flux convergence. It is for these reasons that the upwelling forced by MERRA synoptic waves is weaker and lower than the upwelling forced by tropical waves.

4. Conclusions

We have used a model forced with heating derived from TRMM rainfall rate observations to demonstrate that equatorial waves forced by latent heating drive most of the observed residual mean upwelling across the TTL. Our model simulations produce a residual mean vertical velocity that is essentially the same as values derived from observations within 15° of the equator. Our experimental design has enabled us to isolate equatorial waves from extratropical synoptic waves and determine their relative contribution to driving the upward vertical component of the RMMC. Our estimates show that the upwelling in the TTL driven by equatorial waves is much stronger than the upwelling driven by synoptic waves. The synoptic wave-driven circulation estimated from MERRA reanalysis is confined to much lower altitudes than the tropical wave-driven circulation in our simulations because tropical waves can propagate higher into the TTL and tropical lowermost stratosphere. The EP-flux convergence from synoptic scale waves resides mainly in the troposphere and is therefore not positioned to force residual mean upwelling across the TTL.

Recent work has highlighted the role of synoptic waves in driving future trends in the RMMC in climate models (Shepherd and McLandress, 2011), and the mechanism involves a rising critical level for these waves due to greenhouse-gas-related temperature

changes. Our work does not address these future changes, but examines conditions in the recent past. However, we note that small changes in tropical tropospheric winds on the order of only 5 m s^{-1} have large effects on the tropical wave propagation and TTL upwelling in our model study. This suggests the possibility that small wind biases or differences among climate models could lead to differing conclusions on attribution of wave driving of the TTL upwelling in different models.

We note the TTL upwelling forced by tropical waves in our simulations is largely confined to latitudes within 20° of the equator. Clearly, other waves with extratropical origins and EP flux divergence at subtropical and extratropical latitudes are also important for forcing the full equator-to-pole Brewer-Dobson circulation throughout the stratosphere that is inferred from tracer observations. We highlight here the importance of tropical waves in driving the upwelling within and through the TTL at altitudes, above the influence of latent heating due to convection and below the 70hPa reference level that has been used in many previous model studies (e.g. Butchart et al., 2010). Our results (Figure 8) show that the tropical upwelling driven by tropical quasi-stationary Rossby waves is weak above 100 hPa.

We have also examined the variability of the TTL upwelling throughout a two year simulation that includes two phases of the QBO. Although the TRMM heating that drives the waves has considerable seasonal variability, we found that the circulation driven by the wave response to this heating in a run where the background zonal mean zonal winds were held fixed to zero did not have a regular annual cycle. A strong annual variation in the upwelling is produced when the waves propagate through seasonally variable winds. The maximum upwelling value, averaged within 15° degrees of the equator, varies between $.4 \text{ mm s}^{-1}$ and $.8 \text{ mm s}^{-1}$. When the upwelling is additionally averaged between 90-190 hPa, it varies between $.2 \text{ mm s}^{-1}$ and $.4 \text{ mm s}^{-1}$. The seasonal variation in the subtropical jets modulates the hemisphere in which the strongest EP-flux divergence occurs. A period between June and October when weak mean easterlies occur

over the equator corresponds to weaker wave propagation, EP-flux divergence and RMMC. The variability in TTL upwelling appears to result from relatively large changes in Rossby wave propagation due to only weak variation in tropical wind speed of less than 10 m s^{-1} , with weak westward winds of around 5 m s^{-1} corresponding to the period of weakest upwelling. In addition, variability in the heating appears to be responsible for producing anomalies in the interannual variability of the upwelling (for example, the large upwelling in January 2007).

The mean winds also modify the frequency spectrum of the tropical waves. When the background winds are zero, the portions of the wave spectrum responsible for driving the RMMC are equally split between westward waves with low frequency and stationary waves. With observed background winds, stationary waves are primarily responsible for driving the RMMC. There is still significant wave driving contribution from the transient waves with low frequency. This contribution seems equally split or slightly weighted toward eastward traveling Rossby waves. A downward circulation component due to Kelvin wave driving is detectable in our experiments. Our limited two-year run suggests that the QBO in the lower stratosphere may modulate the Kelvin wave driving near the tropopause, and that this may be the only way that the QBO winds directly affect the TTL upwelling due to tropical waves. Figure 13 summarizes these findings, illustrating the annual variability of the upwelling in relation to the annual variability of the mean winds, and the interannual influence of the QBO on the circulation associated with Kelvin wave damping. We note that while our simplified model approach allows us to isolate the effects of tropical and extratropical waves on TTL upwelling, it cannot address the causes of the annual cycle in the tropical zonal wind itself, which in the real atmosphere results from a balance of eastward and westward accelerations due to tropical waves and the Hadley cell overturning (e.g. Kraucunas and Hartman, 2005).

Acknowledgements

The authors thank Jung-Hee Ryu for providing the stratiform heating algorithm from Ryu et al. (2011). We also thank Ji-Eun Kim and Alison Grimsdell for sharing their archives of TRMM rain rate and infrared cloud height data, respectively. The TRMM rain rate data used in this effort were acquired as part of the activities of NASA's Science Mission Directorate, and are archived and distributed by the Goddard Earth Sciences (GES) Data and Information Services Center (DISC). This work was supported by the NASA Atmospheric Composition: Aura Science Team Program, under Contract No. NNH08CD37C. MJA was also partially supported by contract #NNA10DF70C as part of the Airborne Tropical Tropopause Experiment (ATTREX) under the NASA Earth Venture Program. NCEP Reanalysis data is provided by the NOAA/OAR/ESRL PSD, Boulder, Colorado, USA, from their Web site at <http://www.esrl.noaa.gov/psd/>. MERRA data used in this study/project have been have been provided by the Global Modeling and Assimilation Office (GMAO) at NASA Goddard Space Flight Center through the NASA GES DISC online archive. The comments of two anonymous reviewers made valuable contributions to the manuscript.

5. References

- Abalos, M. W. J. Randel, and E. Serrano, 2012: Variability in upwelling across the tropical tropopause and correlations with tracers in the lower stratosphere, *Atmos. Chem. Phys.*, **12**, 11505-11517.
- Andrews, D. G., J. R. Holton, and C. B. Leovy, 1987: *Middle Atmosphere Dynamics*, Academic, Orlando, FL.
- Boehm, M. T., and S. Lee, 2003: The implications of tropical Rossby waves for tropical tropopause cirrus formation and for the equatorial upwelling of the Brewer–Dobson circulation. *J. Atmos. Sci.*, **60**, 247–261.
- Butchart, N. et al., 2010: Chemistry-Climate Model Simulations of Twenty-First Century Stratospheric Climate and Circulation Changes. *J. Climate*, **23**, 5349-5374.
- Calvo, N., and R. R. Garcia, 2009: Wave forcing of the tropical upwelling in the lower stratosphere under increasing concentrations of greenhouse gases. *J. Atmos. Sci.*, **66**, 3184–3196.
- Calvo, N., R. R. Garcia, W. J. Randel, and D. R. Marsh, 2010: Dynamical mechanism for the increase in tropical upwelling in the lowermost tropical stratosphere during warm ENSO events. *J. Atmos. Sci.*, **67**, 2331–2340. doi: 10.1175/2010JAS3433.1
- Charney, J. G., and P. G. Drazin, 1961: Propagation of planetary-scale disturbances from the lower into the upper atmosphere, *J. Geophys. Res.* **66**, 83-109.
- Deckert, R., and M. Dameris, 2008: Higher tropical SSTs strengthen the tropical upwelling via deep convection. *Geophys. Res. Lett.*, **35**, L10813, doi:10.1029/2008GL033719.
- Dima, I. M., and J. M. Wallace, 2007: Structure of the annual-mean equatorial planetary waves in the ERA-40 reanalyses. *J. Atmos. Sci.*, **64**, 2862–2880.
- Garcia, R. R., and W. J. Randel, 2008: Acceleration of the Brewer–Dobson circulation due to increases in greenhouse gases. *J. Atmos. Sci.*, **65**, 2731–2739.
- Gill, A. E., 1980: Some simple solutions for heat-induced tropical circulation, *Quart. J. R. Met. Soc.* **106**, 447-462.
- Grise, K. M. and D. W. J. Thompson, 2013: On the signatures of equatorial and extratropical wave forcing in tropical tropopause layer temperatures, *J. Atmos. Sci.*, **70**, 1084-1102.
- Holton, J. R., P. H. Haynes, M. E. McIntyre, A. R. Douglass, R. B. Rood, and L. Pfister, 1995: Stratosphere-troposphere exchange. *Rev. Geophys.*, **33** (95RG02097), 403–439.
- Huffman, G. J., R. F. Adler, D. T. Bolvin, G. Gu, E. J. Nelkin, K. P. Bowman, Y. Hong, E. F. Stocker, and D. B. Wolff, 2007: The TRMM Multisatellite Precipitation

- 692 Analysis (TMPA): Quasi-global, multiyear, combined-sensor precipitation estimates
693 at fine scales. *J. Hydrometeorology*, **8**, 38-55.
- 694 Kalnay et al, 1996: The NCEP/NCAR 40-year reanalysis project, *Bull. Amer. Meteor.*
695 *Soc.*, **77**, 437-470.
- 696 Kerr-Munslow, A. M., and W. A. Norton, 2006: Tropical wave driving of the annual
697 cycle in tropical tropopause temperatures. Part I: ECMWF Analyses. *J. Atmos. Sci.*,
698 **63**, 1410–1419.
- 699 Kraucunas, Ian, and D. L. Hartmann, 2005: Equatorial Superrotation and the Factors
700 Controlling the Zonal-Mean Zonal Winds in the Tropical Upper Troposphere. *J.*
701 *Atmos. Sci.*, **62**, 371–389.
- 702 Li, F., J. Austin, and J. Wilson, 2008: The strength of the Brewer-Dobson circulation in a
703 changing climate: coupled chemistry-climate model simulations. *J. Climate*, **21**, 40-
704 57.
- 705 Manabe, S., D. G. Hahn, and J. L. Holloway, Jr., 1974: The seasonal variation of the
706 tropical circulation as simulated by a global model of the atmosphere, *J. Atmos. Sci.*,
707 **31**, 43-83.
- 708 McLandress, C., and T. G. Shepherd, 2009: Simulated anthropogenic changes in the
709 Brewer–Dobson circulation, including its extension to high latitudes. *J. Climate*, **22**,
710 1516–1540. doi: 10.1175/2008JCLI2679.1
- 711 Norton, W. A., 2006: Tropical wave driving of the annual cycle in tropical tropopause
712 temperatures. Part II: Model results. *J. Atmos. Sci.*, **63**, 1420–1431.
- 713 Plumb, R. A., 1979: Eddy fluxes of conserved quantities by small-amplitude waves. *J.*
714 *Atmos. Sci.*, **36**, 1699–1704.
- 715 Plumb, R. A., and J. Eluszkiewicz, 1999: The Brewer–Dobson circulation: dynamics of
716 the tropical upwelling. *J. Atmos. Sci.*, **56**, 868-890.
- 717 Randel, W. J., R. R. Garcia, and F. Wu, 2002: Time-dependent upwelling in the tropical
718 lower stratosphere estimated from the zonal-mean momentum budget. *J. Atmos. Sci.*,
719 **59**, 2141–2152.
- 720 Randel, W. J., R. R. Garcia, and F. Wu, 2008: Dynamical balances and tropical
721 stratospheric upwelling. *J. Atmos. Sci.*, **65**, 3584–3595. doi: 10.1175/2008JAS2756.1
- 722 Randel, W. J., and E. J. Jensen 2013: Physical processes in the tropical tropopause layer
723 and their roles in a changing climate. *Nat. Geosci.*, **6**, 169-176.
- 724 Randel, W. J., and F. Wu, 2006: Biases in stratospheric and tropospheric temperature
725 trends derived from historical radiosonde data. *J. Climate*, **19**, 2094–2104.

- Ryu, Jung-Hee, M. J. Alexander, D. A. Ortland, 2011: Equatorial Waves in the Upper Troposphere and Lower Stratosphere Forced by Latent Heating Estimated from TRMM Rain Rates. *J. Atmos. Sci.*, **68**, 2321–2342. doi: 10.1175/2011JAS3647.1
- Schoeberl, M. R., A. R. Douglass, R. S. Stolarski, S. Pawson, S. E. Strahan, and W. Read, 2008: Comparison of lower stratospheric tropical mean vertical velocities. *J. Geophys. Res.*, **113**, D24109, doi:10.1029/2008JD010221.
- Schumacher, C., R. A. Houze Jr., and I. Kraucunas, 2004: The Tropical Dynamical Response to Latent Heating Estimates Derived from the TRMM Precipitation Radar. *J. Atmos. Sci.*, **61**, 1341–1358.
- Scott, R. K., 2002: Wave-driven mean tropical upwelling in the lower stratosphere. *J. Atmos. Sci.*, **59**, 2745–2759.
- Shepherd, T. G. and C. McLandress, 2011: A Robust Mechanism for Strengthening of the Brewer-Dobson Circulation in Response to Climate Change: Critical-Layer Control of Subtropical Wave Breaking. *J. Atmos. Sci.*, **68**, 784–797.
- Sigmond, M., and J. F. Scinocca, 2010: The influence of the basic state on the Northern Hemisphere circulation response to climate change. *J. Climate*, **23**, doi:10.1029/2008JD009972.
- Solomon, S., K. Rosenlof, R. Portmann, J. Daniel, S. Davis, T. Sanford and G.-K. Plattner, 2010: Contributions of stratospheric water vapor to decadal changes in the rate of global warming. *Science*, **327**(5970), 1219 – 1223.
- Ueyama, R., E. P. Gerber, J. M. Wallace, and D. M. W. Frierson, 2013: The role of high-latitude waves in the intraseasonal to seasonal variability of tropical upwelling in the Brewer-Dobson circulation, *J. Atmos. Sci.*, **70**, 1631–1648.
- Virts, K. S., J. M. Wallace, Q. Fu, and T. P. Ackerman, 2010: Tropical Tropopause Transition Layer Cirrus as Represented by CALIPSO Lidar Observations. *J. Atmos. Sci.*, **67**, 3113–3129.

Figure Captions.

Figure 1. TRMM heating at 7 km and over four seasons in 2007.

Figure 2. Top: The eddy component of the temperature field and zonal and vertical wind components averaged from 10°S-10°N and 2007. The TTL is bounded by the horizontal red lines. Vertical scale of the vectors is exaggerated by a factor of 1000 in this and the following figures. Middle: The eddy component of the temperature field at 26 hPa averaged over 2007. Bottom: The temperature field at 100 hPa averaged over 2007.

Figure 3. EP-flux (vectors) and its divergence (contours) for equatorial waves forced by heating derived from TRMM rainfall, averaged over four seasons in 2007. The results for the simulation with zero background winds are in the left column and for observed background winds in the right column.

Figure 4. Residual mean circulation (vectors) and the residual mean vertical velocity (contours) for equatorial waves forced by heating derived from TRMM rainfall, averaged over four seasons in 2007. The results for the simulation with zero background winds are in the left column and for observed background winds in the right column.

Figure 5. Zonal and monthly mean zonal winds from NCEP for 2006-2007. Top: Vertical profiles averaged from 15°S-15°N, (contour interval 3 ms⁻¹); Bottom: Latitude cross sections averaged from 90-190 hPa (contour interval 4 ms⁻¹).

Figure 6. Zonal and monthly mean vertical component of EP-flux for 2006-2007. Top row: Vertical profiles averaged from 15°S-15°N; Bottom row: Latitude cross sections averaged from 90-190 hPa. Left column: CTRL simulation; Right column: UBR0 simulation.

Figure 7. Same as Fig.6, for EP-flux divergence.

Figure 8. Same as Fig. 6, for vertical residual mean velocity.

Figure 9. EP-flux (vectors) and its divergence (contours) for the DJF 2007 CTRL simulation (left column) and UBR0 simulation (right column). Top row: Stationary waves only. Middle row: Westward waves only. Bottom row: Eastward waves only.

Figure 10. Same as Fig. 9, for the residual mean vertical velocity.

Figure 11. Residual mean vertical velocity averaged over SON and the TTL altitudes. Black curves are for TRMM heating from 2006, red from 2007. Solid curves are for observed background winds from 2006, dashed from 2007. The solid curves show a local minimum near the equator that likely is the result of Kelvin wave forcing.

Figure 12. Response of the TEM model to MERRA transient wave forcing. Top: Residual mean vertical velocity, averaged from 15°S-15°N; Middle: EP-flux (vectors) and its divergence (contours); Bottom: Residual mean circulation (vectors) and residual mean vertical velocity (contours).

Figure 13. Schematic illustrating the annual and quasi biennial influence of tropical waves and TTL upwelling. The color background shows 15S-15N zonal mean winds versus time and height over the two years 2006-2007, with pink shades westerly and blue shades easterly. The TTL region is denoted with dashed black lines. Purple arrows indicate the stationary equatorial Rossby wave-driven upwelling, which is stronger during boreal winter when upper troposphere winds are more westerly, and weaker in boreal summer when winds are more easterly. The smaller red arrows indicate Kelvin wave-driven downwelling, which generally occurs higher in the stratosphere, but can influence the TTL when the QBO westerly winds reach the lower stratosphere.

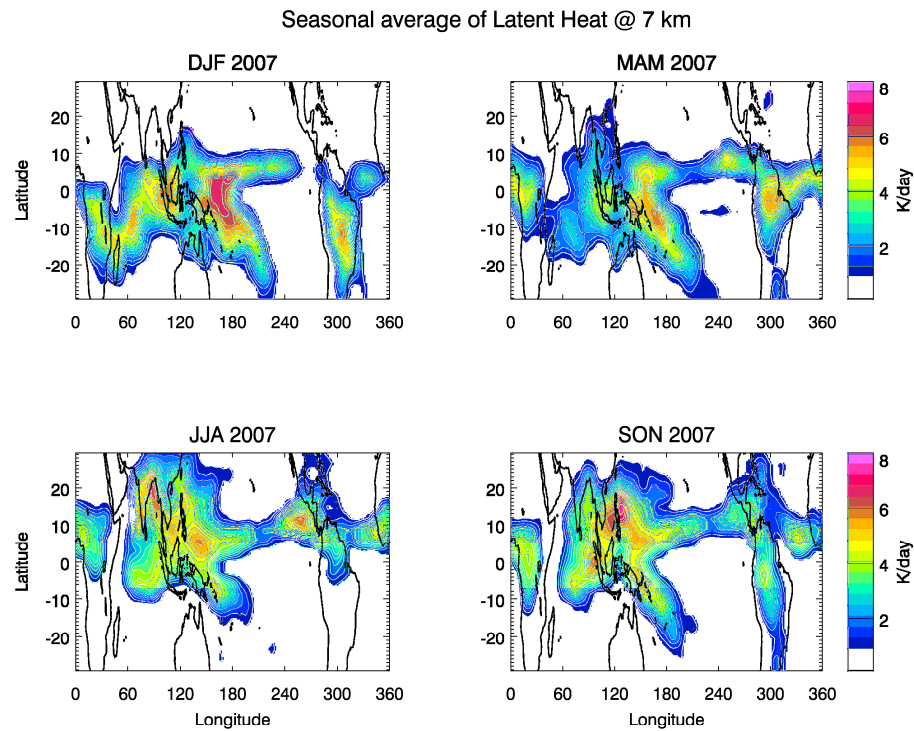


Figure 1. TRMM heating at 7 km and over four seasons in 2007.

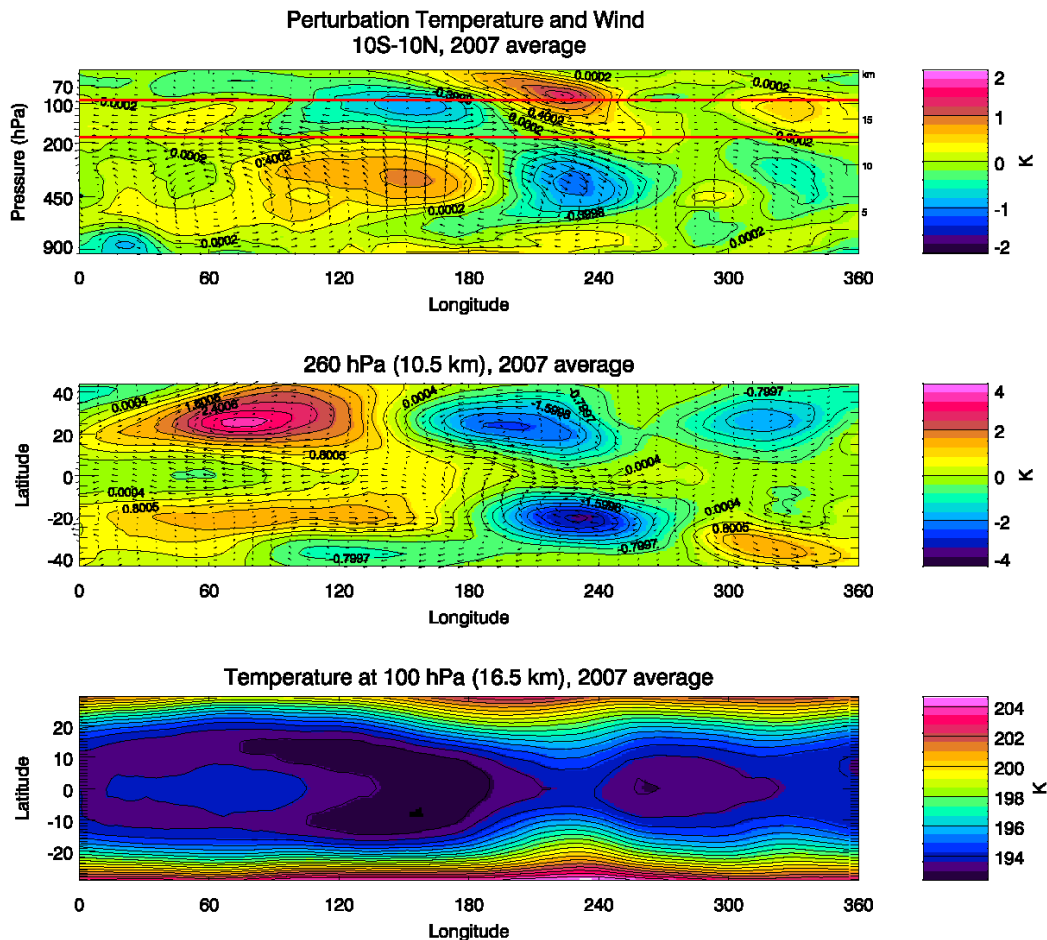


Figure 2. Top: The eddy component of the temperature field and zonal and vertical wind components averaged from 10°S-10°N and 2007. The TTL is bounded by the horizontal red lines. Vertical scale of the vectors is exaggerated by a factor of 1000 in this and the following figures. Middle: The eddy component of the temperature field at 26 hPa averaged over 2007. Bottom: The temperature field at 100 hPa averaged over 2007.

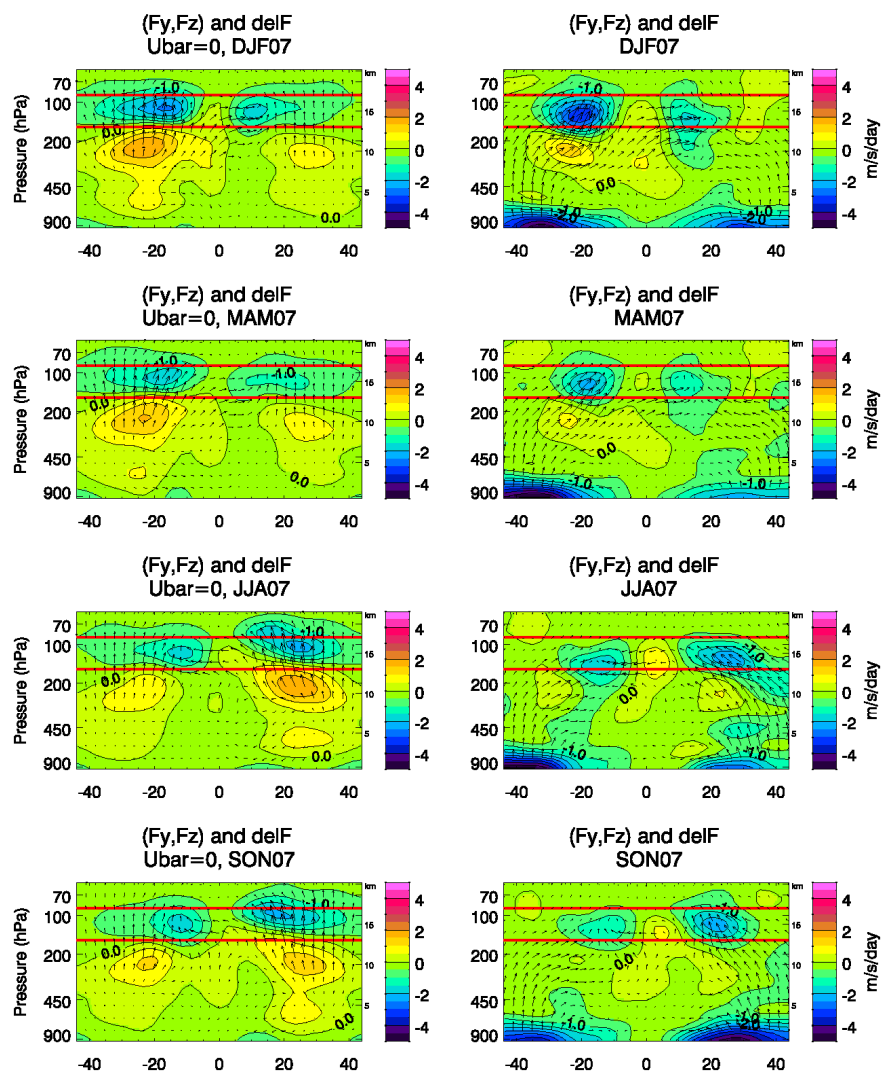


Figure 3. EP-flux (vectors) and its divergence (contours) for equatorial waves forced by heating derived from TRMM rainfall, averaged over four seasons in 2007. The results for the simulation with zero background winds are in the left column and for observed background winds in the right column.

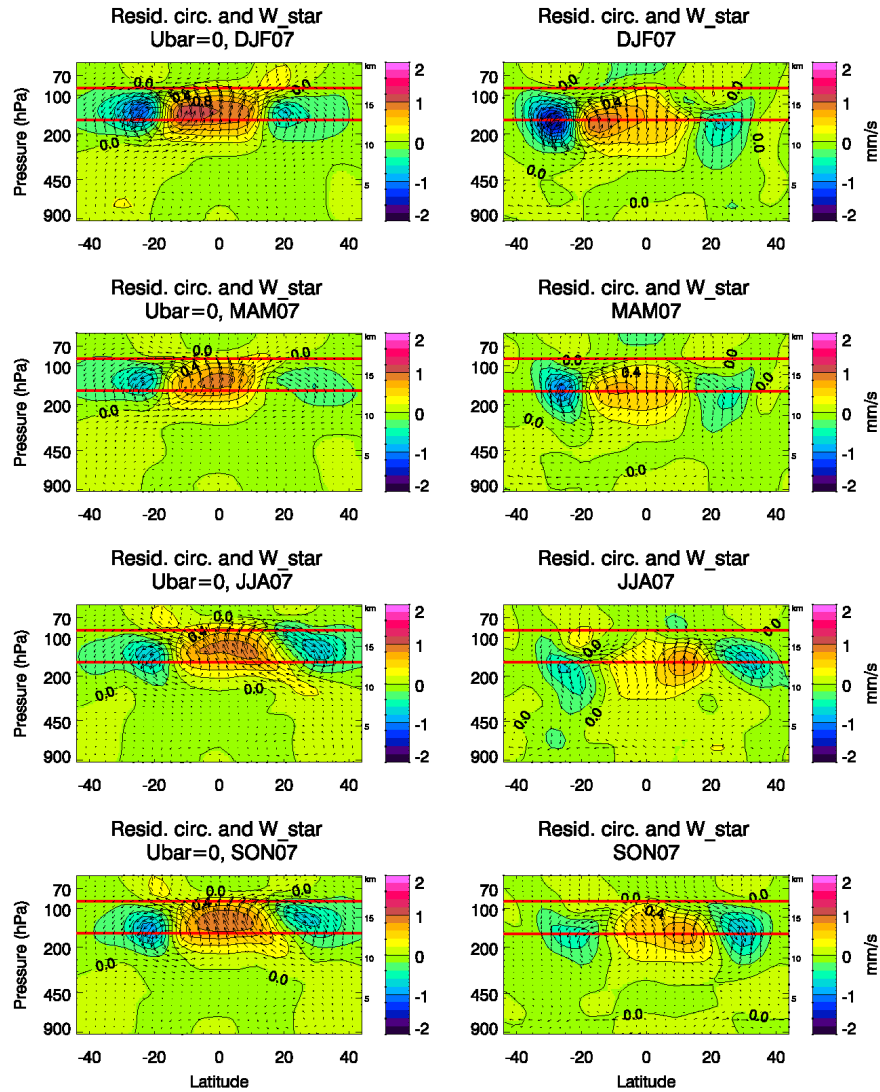


Figure 4. Residual mean circulation (vectors) and the residual mean vertical velocity (contours) for equatorial waves forced by heating derived from TRMM rainfall, averaged over four seasons in 2007. The results for the simulation with zero background winds are in the left column and for observed background winds in the right column.

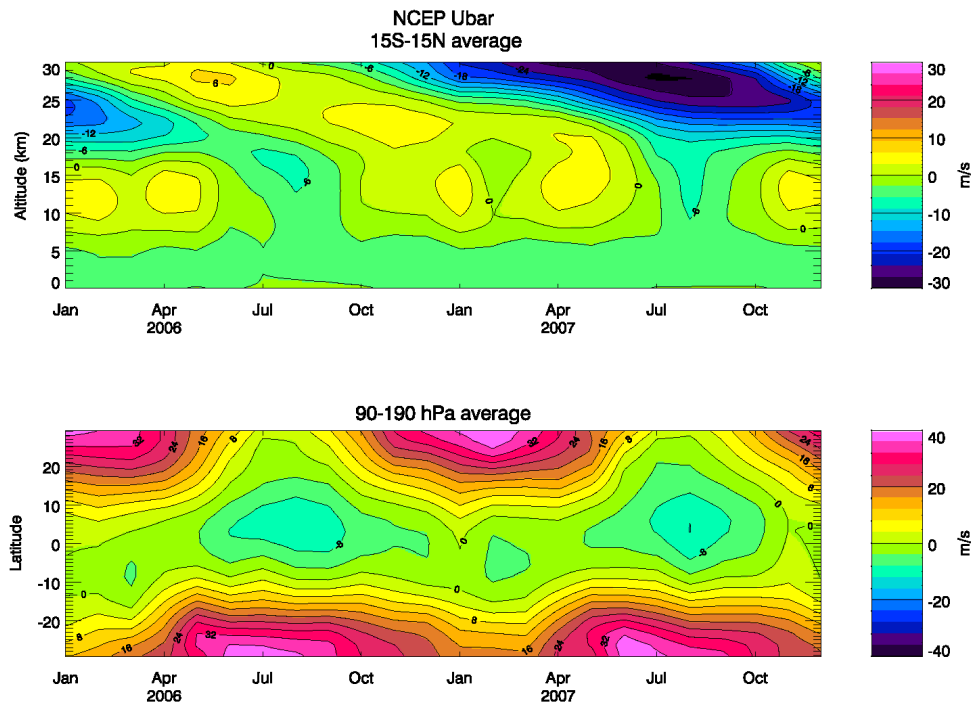


Figure 5. Zonal and monthly mean zonal winds from NCEP for 2006-2007. Top: Vertical profiles averaged from 15°S-15°N, (contour interval 3 ms^{-1}); Bottom: Latitude cross sections averaged from 90-190 hPa (contour interval 4 ms^{-1}).

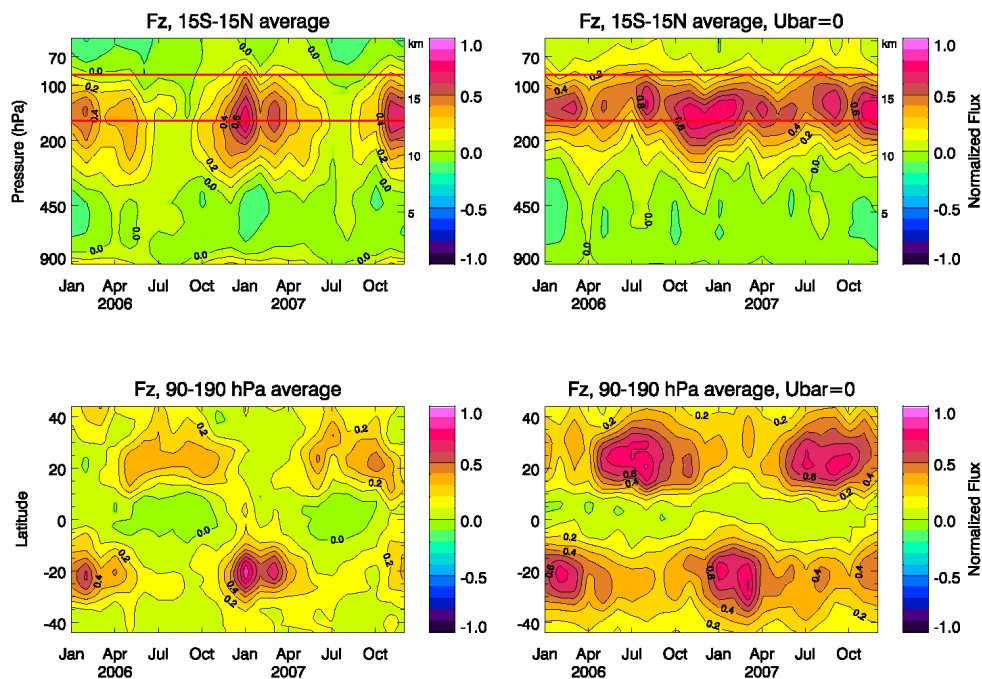


Figure 6. Zonal and monthly mean vertical component of EP-flux for 2006-2007. Top row: Vertical profiles averaged from 15°S-15°N; Bottom row: Latitude cross sections averaged from 90-190 hPa. Left column: CTRL simulation; Right column: UBR0 simulation.

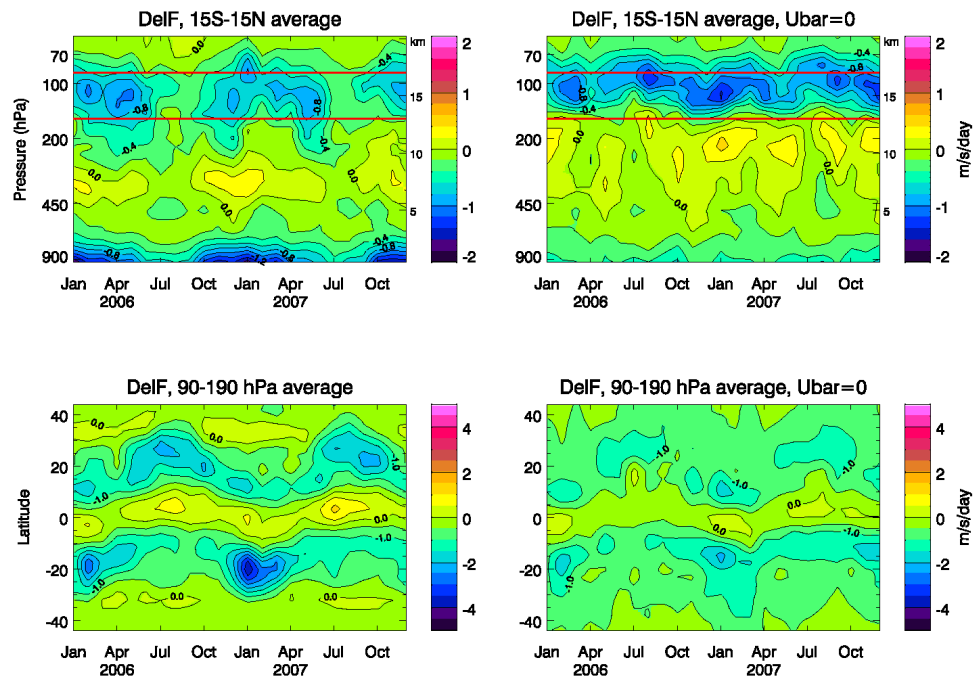


Figure 7. Same as Fig.6, for EP-flux divergence.

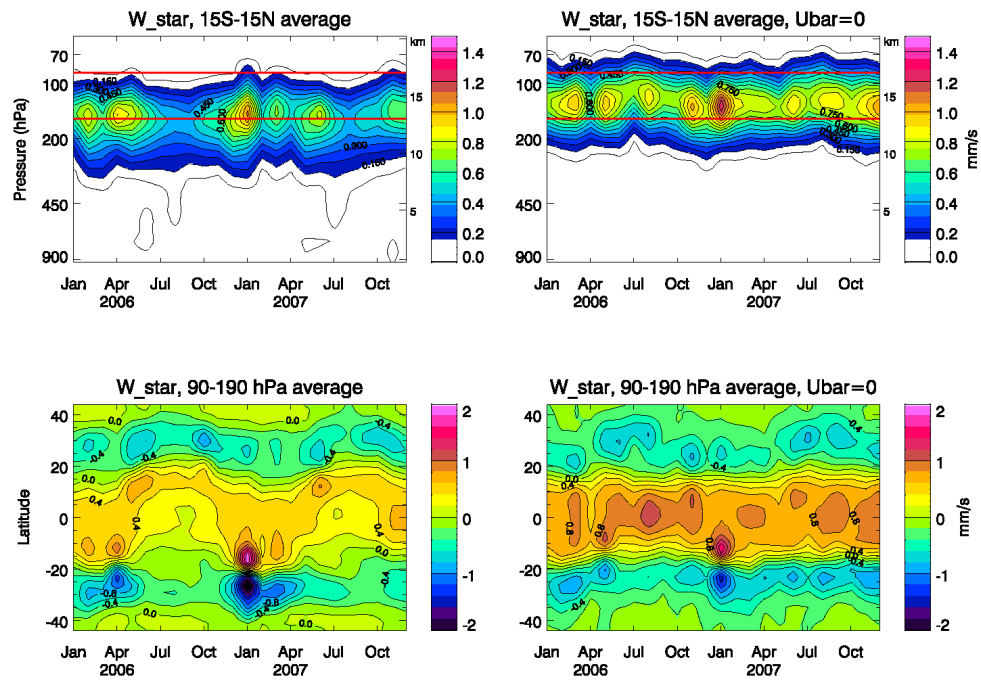
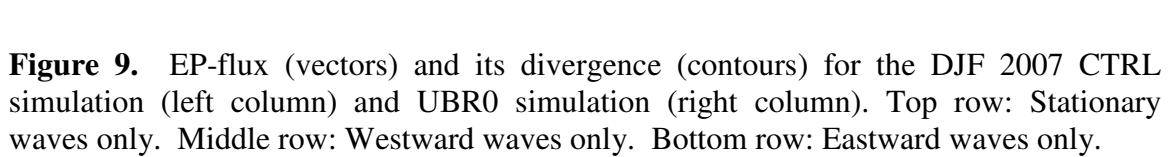


Figure 8. Same as Fig. 6, for vertical residual mean velocity.



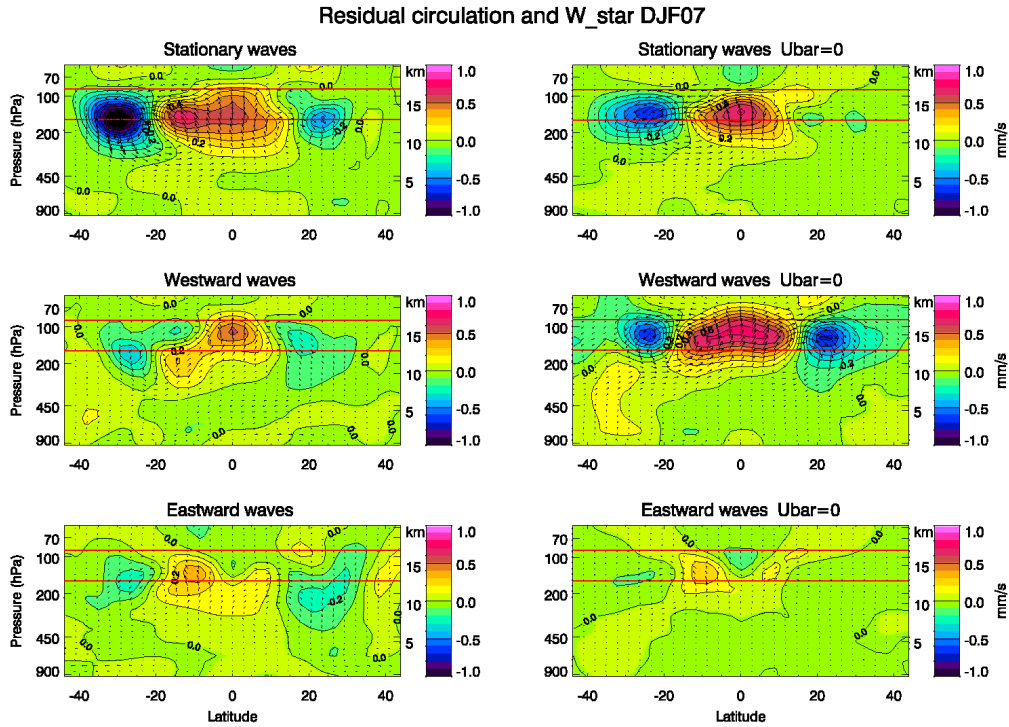
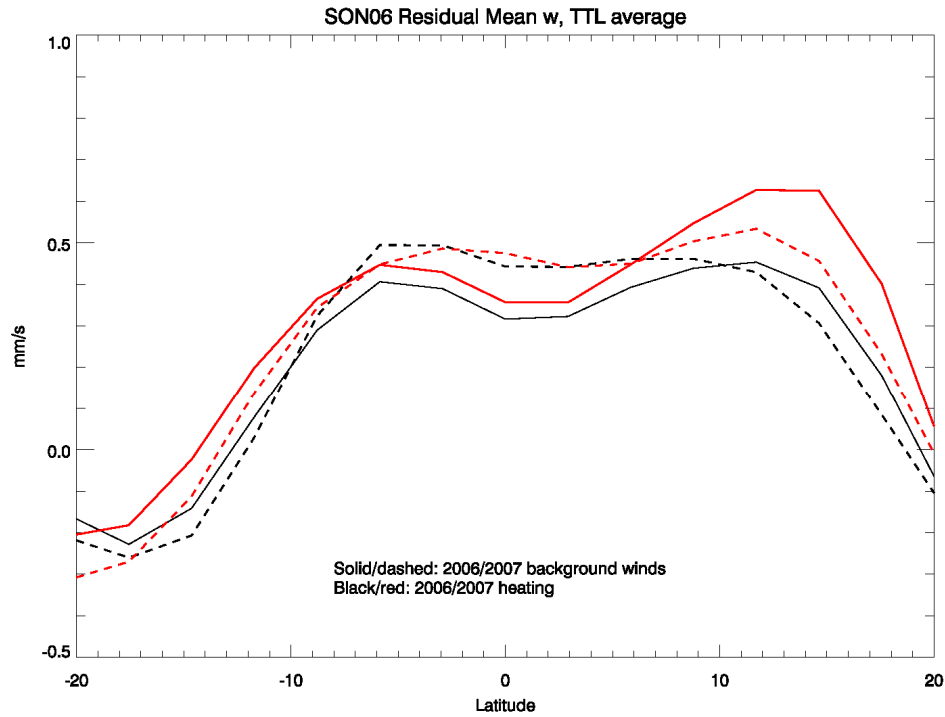


Figure 10. Same as Fig. 9, for the residual mean vertical velocity.



847

848 **Figure 11.** Residual mean vertical velocity averaged over SON and the TTL altitudes.
 849 Black curves are for TRMM heating from 2006, red from 2007. Solid curves are for
 850 observed background winds from 2006, dashed from 2007. The solid curves show a local
 851 minimum near the equator that likely is the result of Kelvin wave forcing.

852

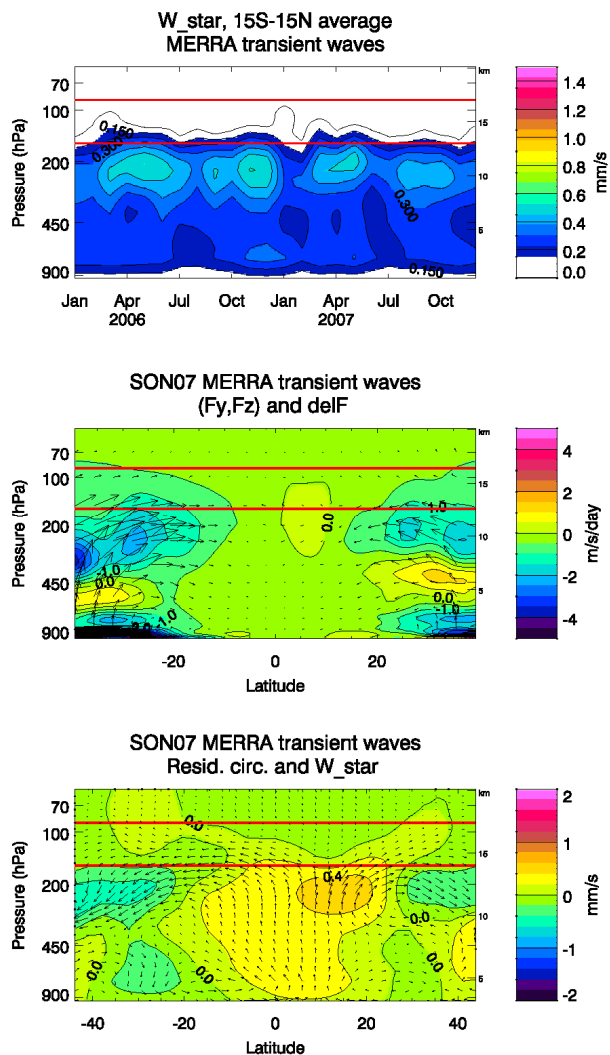
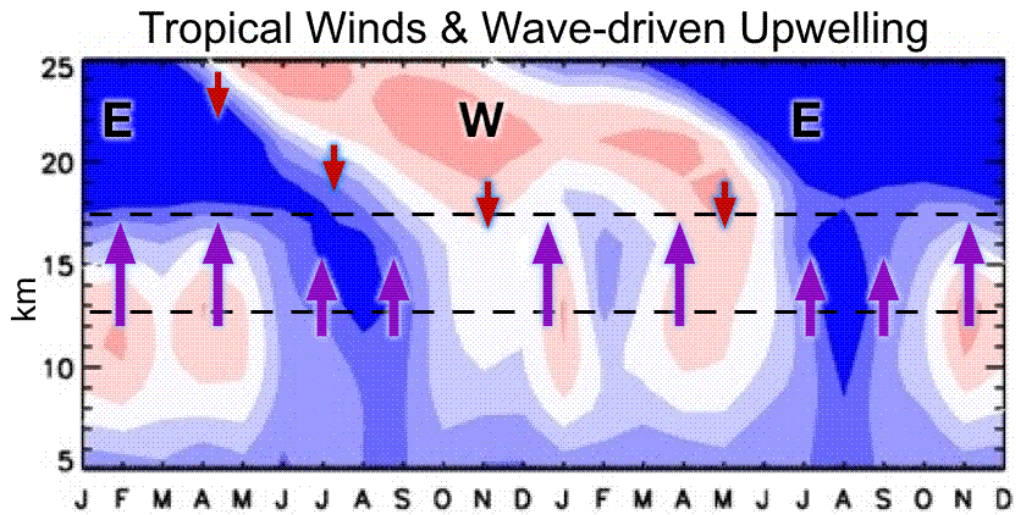


Figure 12. Response of the TEM model to MERRA transient wave forcing. Top: Residual mean vertical velocity, averaged from 15°S-15°N; Middle: EP-flux (vectors) and its divergence (contours); Bottom: Residual mean circulation (vectors) and residual mean vertical velocity (contours).



859

860 **Figure 13.** Schematic illustrating the annual and quasi biennial influence of tropical
861 waves and TTL upwelling. The color background shows 15S-15N zonal mean winds
862 versus time and height over the two years 2006-2007, with pink shades westerly and blue
863 shades easterly. The TTL region is denoted with dashed black lines. Purple arrows
864 indicate the stationary equatorial Rossby wave-driven upwelling, which is stronger
865 during boreal winter when upper troposphere winds are more westerly, and weaker in
866 boreal summer when winds are more easterly. The smaller red arrows indicate Kelvin
867 wave-driven downwelling, which generally occurs higher in the stratosphere, but can
868 influence the TTL when the QBO westerly winds reach the lower stratosphere.